

# In Situ Self-Cross-Linkable, Long-Term Stable Hyaluronic Acid Filler by Gallol Autoxidation for Tissue Augmentation and Wrinkle Correction

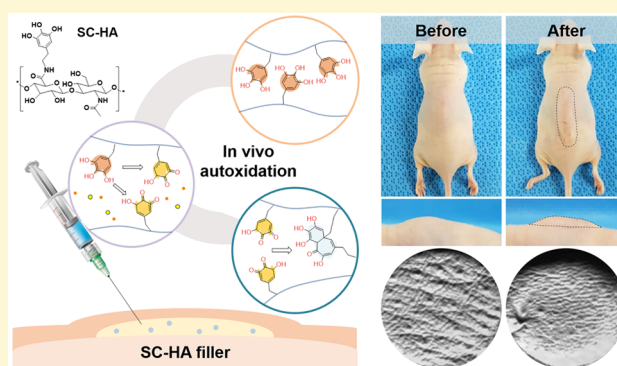
Jung Seung Lee,<sup>†,||</sup> Jung Ho Cho,<sup>†,||</sup> Soohwan An,<sup>†</sup> Jisoo Shin,<sup>†</sup> Soojeong Choi,<sup>†</sup> Eun Je Jeon,<sup>†</sup> and Seung-Woo Cho<sup>\*,†,‡,§</sup>

<sup>†</sup>Department of Biotechnology and <sup>‡</sup>Yonsei-IBS Institute, Yonsei University, Seoul 03722, Republic of Korea

<sup>§</sup>Center for Nanomedicine, Institute for Basic Science (IBS), Seoul 03722, Republic of Korea

## Supporting Information

**ABSTRACT:** Injectable fillers mainly aim to augment tissue volume and correct wrinkles in cosmetic and plastic reconstructions. However, the development of long-lasting, injectable fillers with minimal complications of pain, toxicity, and displacement has been challenging because of the absence of reliable cross-linking chemistry. Here, we report a novel cross-linker-free injectable hydrogel formulated by autoxidation as a highly biocompatible, easily injectable, and long-term volumetrically stable filler agent. Self-cross-linkable hyaluronic acid (SC-HA) with gallol moieties could form a hydrogel via autoxidation of gallols in vivo without additional cross-linking agents. The gelation of SC-HA in situ after injection is accelerated by the self-production of oxygen species and endogenous peroxidase in vivo. The SC-HA filler does not require a high injection force, thus minimizing pain, bleeding, and tissue damage-associated complications. In addition, improved tissue adhesiveness of the SC-HA hydrogel by oxidized gallols (shear strength; 2 kPa) prevented displacement of the filler constructs from the injection site. The SC-HA filler retained its mechanical properties in vivo (600–700 Pa) for wrinkle correction and volumetric augmentation up to 1 year after injection. Overall, the performance of the SC-HA hydrogel as an injectable dermal filler was superior to that of commercially available, chemically cross-linked biphasic HA filler composites in terms of injectability, tissue adhesiveness, and long-term volumetric augmentation. Our injectable HA hydrogel with no need of cross-linkers provides a long-lasting filler that has clinical utility for cosmetic applications.



## INTRODUCTION

Hydrogels have diverse applications in biomedical engineering fields, which include drug delivery, surface modification, tissue adhesives, and tissue engineering scaffolds.<sup>1–3</sup> In particular, injectable hydrogels accommodate facile and minimally invasive procedures for site-directed implantation of three-dimensional constructs.<sup>4–6</sup> With the huge interest in antiaging and cosmetic applications, the market for injectable fillers composed of polymeric hydrogels has exponentially increased in recent years. Filler composites can be utilized for cosmetic purposes, for volumetric recovery after loss or resection of soft tissues,<sup>7,8</sup> and for the medical treatment of human immunodeficiency virus-associated facial lipoatrophy.<sup>9,10</sup> Recent advances in material science and clinical techniques have provided diverse options for volumetric tissue augmentation. Injectable bulking agents made of various synthetic and natural polymers, such as silicon, polycaprolactone, calcium hydroxyapatite, collagen, and decellularized matrix, have been used clinically.<sup>11–14</sup> However, long-term inflammation, allergic reactions, and rapid degradation due to weak mechanical

properties have limited the widespread use of the current materials as filler composites.<sup>15–18</sup>

Hyaluronic acid (HA), a primary component of extracellular matrices in skin and various connective tissues, is regarded as one of the best ingredients to fabricate injectable fillers owing to its biocompatibility and low immunogenicity.<sup>19–21</sup> In addition, HA-based fillers can be removed through enzymatic degradation using hyaluronidase when unexpected events, such as displacement and side effects, occur.<sup>19,20</sup> HA-based filler composites can be categorized into monophasic and biphasic types, according to their chemical and physical formulation. Monophasic HA fillers can be homogeneously injected, but they usually show a low volumetric augmentation effect and short retention time due to their weak mechanical properties.<sup>22–24</sup> Although the mechanical stability of monophasic HA fillers can be improved by increasing the cross-linking density

Received: July 15, 2019

Revised: November 7, 2019

Published: November 21, 2019

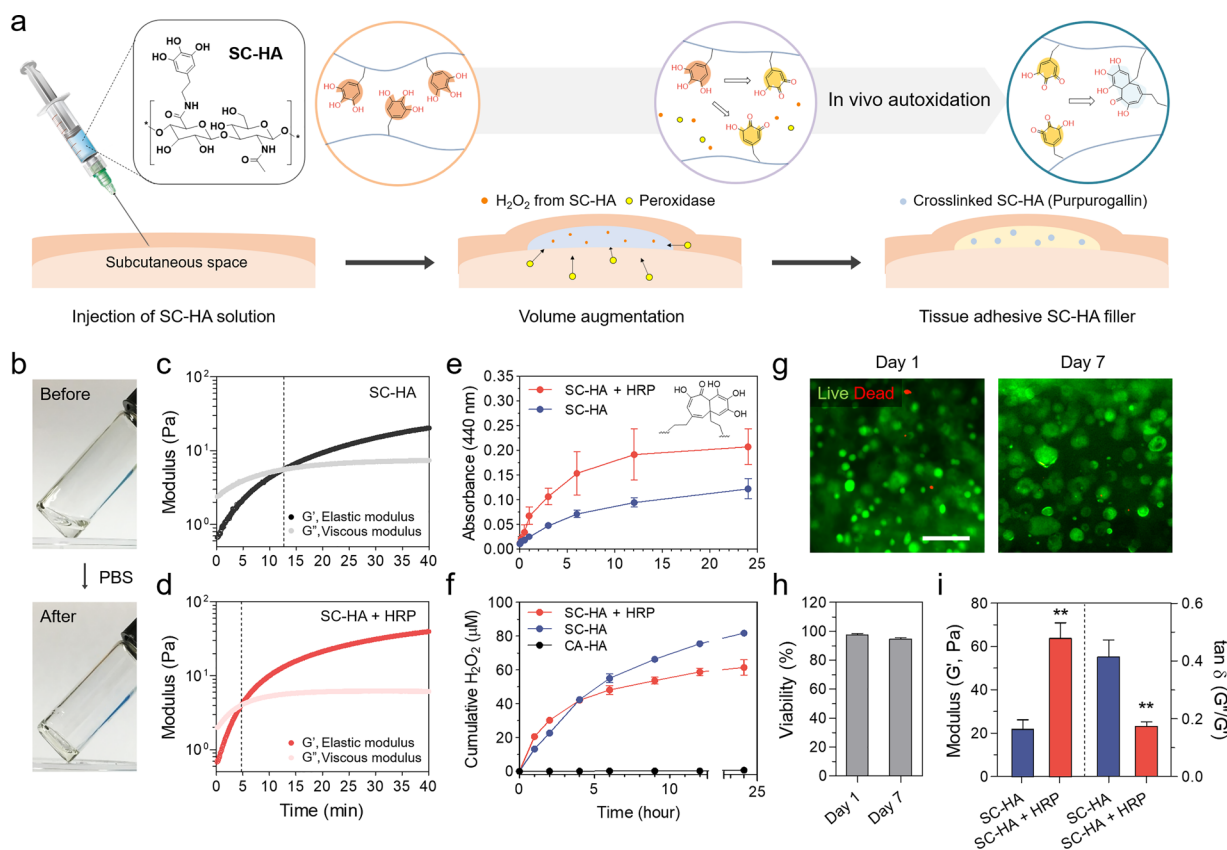


**Figure 1.** Preparation and characterization of the SC-HA hydrogel. (a) Schematic illustration demonstrating the in vivo cross-linking mechanism of the SC-HA hydrogel via autoxidation of gallol groups by endogenous peroxidase in tissues and hydrogen peroxide (H<sub>2</sub>O<sub>2</sub>) generated from oxidized SC-HA for volumetric tissue augmentation. (b) Gross view of SC-HA before and after gelation. Gelation kinetics of the SC-HA hydrogel (c) without or (d) with horseradish peroxidase (HRP). The dashed lines indicate the time of hydrogel formation when G' (elastic modulus) and G'' (viscous modulus) crossed. (e) Change in absorbance value at 440 nm of SC-HA solution with (red) or without (blue) HRP over time (*n* = 3). (f) Quantification of generated H<sub>2</sub>O<sub>2</sub> during the gelation process of SC-HA with (red) or without (blue) HRP (*n* = 3). Catechol-conjugated HA (CA-HA) was used as a control. (g, h) In vitro biocompatibility test by Live/Dead staining of human dermal fibroblasts (HDFs) encapsulated in the SC-HA hydrogel (cross-linked by 0.06 U mL<sup>-1</sup> HRP) after 1 and 7 days of culture. Scale bar is 100 μm. (i) Elastic modulus at 1 Hz and elasticity (tan δ, G''/G') of SC-HA hydrogels (*n* = 4, \*\*; *p* < 0.01, compared to the SC-HA group).

and molecular weight of the composites, a larger-size needle is required to compensate for the higher extrusion force during injection by the increased viscosity, which is closely related to acute pain.<sup>25,26</sup> In contrast, biphasic HA fillers containing specific size cross-linked HA particulates with noncross-linked HA solution maintain better stability in vivo.<sup>24</sup> Chemically cross-linked particulates of biphasic fillers provide enhanced elasticity and better performance in volume maintenance compared with monophasic fillers, but they often form inhomogeneous shapes that roughen the injection site and are prone to displacement due to the weak polymeric network within the composite.<sup>27,28</sup> In addition, chemical reagents for HA cross-linking, such as glutaraldehyde, butanediol-diglycidyl ether (BDDE), 1,2,7,8-diepoxyoctane, and divinyl sulfone, can pose safety concerns involving inflammation, foreign body reaction, and toxicity after injection.<sup>29,30</sup> Therefore, there is a huge need to develop an advanced cross-linking system that provides a safe, long-lasting, and highly usable filler composite.

In this study, we developed a self-cross-linkable HA (SC-HA) filler without cross-linkers to overcome rheological and physiological limitations and safety issues of the current HA cross-linking systems. The SC-HA hydrogel was prepared by adopting the phenolic oxidation process to HA polymerization. Inspired by the strong underwater adhesion and rapid self-

regeneration of marine organisms, phenolic compounds have been widely used in cross-linking chemistry to develop functional hydrogel systems for various biomedical applications.<sup>31–35</sup> In particular, the gallol moiety that contains three hydroxyl groups on the benzene ring generates a dimerized form of intermediates during the oxidation process, leading to spontaneous cross-linking and high affinity to various proteins.<sup>36–38</sup> In addition, previous studies have reported that the strong oxidative property of the gallol group induces rapid gelation kinetics, especially when catalysts (e.g., sodium hydroxide, sodium periodate, peroxide) are supplemented during the cross-linking process.<sup>39,40</sup> Therefore, we assumed that a gallol-modified-HA conjugate could be readily injected as a viscous solution and subsequently undergo rapid cross-linking via autoxidation reaction mediated by oxygen species released from oxidized gallol groups and innate oxidative enzymes (e.g., endogenous peroxidases) even without cross-linking agents, enabling long-term stable volumetric tissue augmentation (Figure 1a). Here, we also explored the mechanism of in vivo cross-linking of the SC-HA hydrogel by gallol oxidation and demonstrated its extraordinary properties as a dermal filler for successful application in volumetric tissue augmentation. The SC-HA filler was validated as a functional alternative that overcomes the

limitations of conventional monophasic and biphasic HA fillers in terms of injectability, biocompatibility, adhesiveness, and long-term performance.

## ■ EXPERIMENTAL SECTION

**Synthesis and Cross-Linking of SC-HA.** SC-HA was synthesized by conjugating a gallol moiety to the HA backbone as we previously described.<sup>39</sup> Briefly, HA (molecular weight 200 kDa and 1 MDa; Lifecore Biomedical, Chaska, MN) was fully dissolved (1%, w/v) in triple-distilled water (TDW). 1-(3-Dimethylaminopropyl)-3-ethylcarbodiimide hydrochloride (EDC; Thermo Fisher Scientific, Waltham, MA) and *N*-hydroxysuccinimide (Sigma-Aldrich, St. Louis, MO) were added at molar ratios of 1.5:1 and 1:1 to HA, respectively, and reacted for 30 min. Then, 5'-hydroxydopamine (Sigma-Aldrich) was added at a molar ratio of 1:1 to HA, and the pH was adjusted to 4.5. After an overnight reaction, the reactant was dialyzed in acidic phosphate-buffered saline (PBS, pH 4.5) and TDW using a Cellu-Sep dialysis membrane (Membrane Filtration Products Inc., Seguin, TX) with a 6–8 kDa cutoff, to remove unreacted chemicals. The resulting conjugate was lyophilized and stored at  $-80^{\circ}\text{C}$  until use. Catechol-modified-HA (CA-HA) was synthesized as previously described.<sup>32</sup> To confirm the conjugation of the gallol group, the synthesized SC-HA conjugate was dissolved in deuterium oxide (Sigma-Aldrich) and then analyzed using proton nuclear magnetic resonance ( $^1\text{H NMR}$ ) spectroscopy at 300 MHz (Bruker, Billerica, MA). The conjugation efficiency, expressed as the ratio of the modified carboxyl group in HA unit with the gallol group, was calculated by dissolving the SC-HA conjugate (1 mg mL<sup>-1</sup>) in acidic PBS (pH 5) and measuring the absorbance at 280 nm using ultraviolet–visible (UV–vis) spectroscopy (JASCO Corporation, Tokyo, Japan). Serially diluted 5'-hydroxydopamine (maximum concentration 1 mg mL<sup>-1</sup>) was used to construct a standard curve. To initiate cross-linking, the SC-HA conjugate was dissolved in PBS under ambient air condition, and horseradish peroxidase (HRP, 0.06 U mL<sup>-1</sup>; Sigma-Aldrich) was added to the dissolved conjugate solution to model the peroxidase-mediated oxidation occurring *in vivo*. The change in the absorption spectrum during gelation was examined by using UV–vis spectroscopy (JASCO Corporation) at predetermined time points (1, 10, and 60 min and 3, 6, 12, and 24 h). In all experiments, SC-HA was dissolved at a concentration of 2% (w/v), and 0.06 U mL<sup>-1</sup> HRP (final concentration) was used, unless otherwise stated. Because the dissolution of the SC-HA conjugate would affect homogenous gelation and subsequent *in vivo* cross-linking of SC-HA,<sup>41</sup> the dissolution process was optimized to minimize unwanted oxidation of the SC-HA conjugate before injection. In brief, SC-HA solution was vigorously vortexed for 10 min to promote dissolution of the SC-HA conjugate in PBS, centrifuged to remove bubbles in the pregel solution, and immediately used for analyses or injection experiments.

**Quantification of Hydrogen Peroxide (H<sub>2</sub>O<sub>2</sub>).** The SC-HA conjugate was dissolved at 2% (w/v) concentration in PBS (Sigma-Aldrich) and was either not supplemented or supplemented with HRP (0.06 U mL<sup>-1</sup>). Aliquots of 50  $\mu\text{L}$  were added to conical tubes. CA-HA dissolved in PBS at 2% (w/v) concentration was used as a control. After cross-linking in ambient air condition, 100  $\mu\text{L}$  of 0.2 M hydrochloride (Sigma-Aldrich) solution was added to the tubes to stop the autoxidation process at predetermined time points. After incubation at room temperature for 30 min, the samples were stored at  $-20^{\circ}\text{C}$  until analysis. The amount of generated H<sub>2</sub>O<sub>2</sub> was calculated using a Pierce quantitative peroxidase assay kit (Thermo Fisher Scientific).

**Rheometric Analysis and Adhesiveness Measurement.** A commercially available biphasic HA filler composite (Restylane Perlane Lidocaine; Q-Med, Uppsala, Sweden) was used as a control. A rotating rheometer (Anton Paar, Ashland, VA) was used to evaluate oscillatory rheological properties. To observe the gelation kinetics of SC-HA hydrogels, the conjugate was immediately dissolved in PBS (2%, w/v) that was not supplemented or supplemented with HRP (0.06 U mL<sup>-1</sup>) and placed between the plate and probe. The storage modulus ( $G'$ ) and loss modulus ( $G''$ ) were recorded in a time sweep

mode (strain: 10%; frequency: 1 Hz). The viscoelastic modulus of the SC-HA hydrogel and the conventional HA filler was determined by measuring  $G'$  and  $G''$  in a frequency sweep mode (strain: 10%; frequency: 0.1–1 Hz). For the evaluation of the *in vitro*-cross-linked hydrogel, the SC-HA conjugate dissolved in PBS (2%, w/v) in the absence or presence of HRP (0.006, 0.06, 0.6, or 6 U mL<sup>-1</sup>) was self-cross-linked for 3 h in a humidified chamber to prevent the hydrogels from drying during gelation. The viscoelastic modulus of the *in vivo*-cross-linked SC-HA hydrogel (2%, w/v) was examined using the retrieved hydrogel constructs from subcutaneous spaces of ICR mice (OrientBio, Seongnam, Gyeonggi-do, Korea) at several time points. The value of  $G''/G'$  at 1 Hz was defined as elasticity ( $\tan \delta$ ). The viscosities of PBS, commercial HA filler, and SC-HA filler (2%, w/v) were measured in the steady shear sweep mode (0.1–1000 s<sup>-1</sup>) using a rheometer (Anton Paar). To compare the adhesiveness of the SC-HA hydrogel (2%, w/v) cross-linked with HRP (0.06 U mL<sup>-1</sup>) and the commercial HA filler, the samples were placed between mouse skin tissues tightly attached to a base plate and probe, and the detachment stress was recorded using the tack test mode of a rheometer (Anton Paar) by pulling the probe at a speed of 10  $\mu\text{m s}^{-1}$ . For the lap shear test, skin tissues (1 cm  $\times$  1 cm) were fixed on glass slides, and each filler composite was placed between tissues. After 3 h of incubation in a humidified chamber, the shear strength was measured using an OTT-001 universal testing machine (UTM) (Oriental TM, Siheung, Korea) by pulling the glass slides at a rate of 1 mm s<sup>-1</sup>.

**Swelling Test.** To evaluate the swelling property of HA hydrogels, fully cross-linked CA-HA and SC-HA hydrogels (2%, w/v) were incubated in PBS at 37  $^{\circ}\text{C}$  and retrieved for measuring the weight at several time points. SC-HA hydrogels were cross-linked in the absence or presence of HRP (0.06 or 0.6 U mL<sup>-1</sup>). The swelling ratio was calculated by the following formulation:  $(W_t - W_i)/W_i \times 100$ , where  $W_t$  and  $W_i$  represent the weight of the hydrogel at each time point and the weight of the hydrogel before immersion in PBS, respectively ( $n = 3-4$ ).

**Cell Culture.** The biocompatibility of the SC-HA hydrogel filler was evaluated by culturing human dermal fibroblasts (HDFs) in the hydrogels. For cell encapsulation, HDFs were mixed with 2% (w/v) SC-HA pregel solution (in PBS) supplemented with HRP (0.06 and 0.6 U mL<sup>-1</sup>) at a density of  $1 \times 10^7$  cells mL<sup>-1</sup>. The pregel solution was allowed to undergo autoxidation in a humidified ambient air condition at 37  $^{\circ}\text{C}$ . The fully cross-linked hydrogels were incubated in Dulbecco's modified Eagle's medium (Thermo Fisher Scientific) supplemented with 10% (v/v) fetal bovine serum (Thermo Fisher Scientific) and 1% (v/v) penicillin/streptomycin (Gibco, Gaithersburg, MD). After 1 and 7 days of *in vitro* culture, cells in SC-HA hydrogels were stained with a Live/Dead viability/cytotoxicity kit (Invitrogen, Carlsbad, CA) and visualized by fluorescence microscopy using a model IX71 microscope (Olympus, Tokyo, Japan). The viability of the encapsulated cells was calculated by image-based counting of live (green) and dead (red) cells.

**Injectability Test.** The injectability of each HA filler was evaluated by comparing the force required for injection. Briefly, the SC-HA conjugate (200 K, 1 M) dissolved in PBS (2%, w/v) and the commercial biphasic HA filler (Restylane, 1 M) were used to individually fill a 1 mL syringe of different needle gauges (25, 27, 29, or 30 G). The extrusion force was measured by UTM with a 10 kg load cell. The syringes containing each filler composite were compressed by a cylindrical bar that was fixed on the UTM with a customized immovable jig, and the probe was moved at a rate of 12.5 mm s<sup>-1</sup>. The break loose force was defined as the force needed to initiate the movement of plunger, and the dynamic glide force was considered as the force needed to sustain the movement of plunger after the initiation of movement.

**In Vivo Experiment with HA Filler.** To inject each filler composite, 5 week-old ICR hairless male mice (OrientBio) were anesthetized with ketamine (100 mg kg<sup>-1</sup>, Yuhan, Seoul, Korea) and xylazine (20 mg kg<sup>-1</sup>, Bayer Korea, Ansan, Korea). One hundred microliters of the commercial HA filler (Restylane, 1 M) or the SC-HA hydrogel filler (200 K, 1 M) (2% (w/v) conjugate dissolved in

PBS) were injected into subcutaneous spaces of mice. To monitor the displacement of the HA filler composite, the center of each filler at the initial injection site was marked and tracked every week for 4 weeks. The displacement distance was determined by calculating the distance from the initial position at several time points using ImageJ software (National Institutes of Health, Bethesda, MD). In vivo retention and long-term stability of the injected HA fillers were examined by measuring the wet weight and dimensions with an electronic scale and caliper rule, respectively, after carefully retrieving the filler constructs at predetermined time points (0, 1, and 2 weeks, and 1, 2, 3, 6, and 12 months). The volume ( $V$ ) of the retrieved fillers was calculated as  $V = 4\pi/3 \times \text{length} \times \text{width} \times \text{height}$ . Remnant volume and weight were normalized with those at the initial time point. In vivo biocompatibility of the injected SC-HA filler was confirmed by histological analysis. The extracted samples were fixed with 4% (w/v) paraformaldehyde (Sigma-Aldrich), embedded in paraffin, sectioned (6  $\mu\text{m}$  thick), and stained with hematoxylin and eosin (H&E) and toluidine blue to check the inflammatory response. The samples were also stained with primary antibodies against keratin 5 (1:100 dilution, Abcam, Cambridge, U.K.) and F4/80 (1:100 dilution, Abcam) and then immunofluorescently stained with Alexa 488- or 594-conjugated secondary antibodies (1:200 dilution, Invitrogen). The counterstaining for cell nuclei was conducted with 4',6-diamidino-2-phenylindole (Vector Laboratories, Burlingame, CA).

**Wrinkle Study.** A mouse model of wrinkles was used. Wrinkling was induced by treating 6 week-old ICR hairless mice (Orientbio) with calcitriol (1 $\alpha$ ,25-dihydroxyvitamin D3, Sigma-Aldrich). Calcitriol solution (0.2  $\mu\text{g}$  dissolved in 100  $\mu\text{L}$  of ethanol) was gently spread on mouse dorsal skin five times a week for 6 weeks. After 2 weeks of recovery, commercial HA filler (Restylane), SC-HA filler [2% (w/v) dissolved in PBS], and SC-HA filler supplemented with epidermal growth factor (EGF, 10  $\mu\text{g}$  per injection; R&D Systems, Inc., Minneapolis, MN) were subcutaneously injected for tissue augmentation and wrinkle correction. Wrinkle images were acquired using a charge-coupled device camera (12 MP, f/1.8, Largan Precision, Taichung, Taiwan) before and after filler injection, and wrinkle surface area was evaluated by using an image analysis program (ImageJ, National Institutes of Health, Bethesda, MD). The taken images were also used for scoring evaluation according to the classification criteria established from a previous study (0, no wrinkles; 1, just perceptible wrinkles; 2, mild and shallow wrinkles; 3, moderate deep wrinkles; 4, deep wrinkles with well-defined edges; 5, severe and very deep wrinkles with redundant fold).<sup>42</sup> The randomized images of each group ( $n = 6-8$ ) were exposed without any information about the group, and the scores from the blinded investigators ( $n = 15$ ) were averaged for the assessment. For further evaluation of wrinkle correction, wrinkle morphology was replicated using silicone-based replicas (Silflo; J&S Davis, Stevenage, U.K.) before and after filler injection and was analyzed using a Visioline VL 650 skin visiometer (Courage-Khazaka Electronic GmbH, Koln, Germany). Imaging of the wrinkle surface and quantitative indexes including area, length, and depth were evaluated using the Quantirides system (Monaderm, Monaco, France). To check the effect of the EGF-incorporating SC-HA filler, skin tissue adjacent to the injected HA filler was examined with H&E and Masson's Trichrome staining 1 month after the injection.

**Growth Factor Release Test.** To check growth factor release from SC-HA hydrogels, recombinant human EGF protein (R&D Systems) was added into the SC-HA pregel solution, cross-linked in the presence of HRP (0.6 U mL<sup>-1</sup>), and then the resultant hydrogels containing EGF were incubated in PBS at 37 °C. The final concentration of the hydrogel was 2% (w/v), and 10  $\mu\text{g}$  of EGF was incorporated within the hydrogel. To gradually degrade the SC-HA hydrogel, 0.5 U mL<sup>-1</sup> hyaluronidase (Sigma-Aldrich) was treated during the incubation. PBS was harvested at predetermined time points (8 h, day 1, day 2, day 3, day 5, and day 7), and the released EGF in the retrieved PBS was quantified using an enzyme-linked immunosorbent assay (ELISA) kit for human EGF (Duo Set, R&D Systems) following the manufacturer's instruction.

**Statistical Analysis.** All of the quantitative data are presented as mean  $\pm$  standard deviation. Statistical analysis was performed with GraphPad Prism 5 software (GraphPad Software, San Diego, CA) using unpaired Student's *t*-test. Differences between groups represented by *p*-values <0.05 and 0.01 were considered statistically significant.

## RESULTS AND DISCUSSION

The gallol modification of the SC-HA hydrogel resulted in the formation of a cross-linker-free HA hydrogel by enzymatic autoxidation. The SC-HA conjugate (200 kDa HA) was synthesized by coupling gallol-containing 5'-hydroxydopamine to the HA backbone by carbodiimide chemistry (Figure S1a). The success of the conjugation was confirmed by <sup>1</sup>H NMR spectroscopy, which demonstrated newly detected peaks at 2.8 and 6.5 ppm. The peaks represent ethyl protons (between gallol and amine groups) and aromatic protons (Figure S1b). The conjugation efficiency, defined as the ratio of the modified HA unit with the gallol group, was 8.3%. The stable SC-HA hydrogel was formed by merely dissolving the conjugate in neutral PBS (pH 7.4) at 2% (w/v) concentration, without addition of any catalysts or change of physiological conditions, such as pH and temperature (Figure 1b). Through the autoxidation of the SC-HA conjugate in a pregel solution, the oxidized gallol groups gradually cross-linked themselves, and the resultant hydrogel was formed approximately 13 min after the dissolution in PBS, which was indicated by the cross-over time between  $G'$  (elastic modulus) and  $G''$  (viscous modulus) (Figure 1c). Given that endogenous peroxidases in tissue and body fluid can act as catalytic enzymes for autoxidation when the pregel solution of SC-HA is administered in vivo,<sup>40</sup> HRP was used as a model enzyme to recapitulate the cross-linking process in vivo. Addition of HRP (0.06 U mL<sup>-1</sup>) to the SC-HA pregel solution shortened the cross-linking time to 5 min (Figure 1d), supporting our hypothesis of the accelerated gelation kinetics of SC-HA by enzymatic autoxidation. UV-vis spectroscopy analysis was also performed to evaluate the cross-linking mediated by gallols within the hydrogel. After initiating auto-cross-linking of the SC-HA conjugate, there was a gradual increment of absorbance in a broad range from 280 to 440 nm, resulting from various oxidative intermediates and purpur-ogallins formed by the dimerization of gallols (Figure S2). When HRP was supplemented in the SC-HA pregel solution, the overall absorbance value was increased much faster than that of SC-HA without the enzyme, indicating accelerated autoxidation by the enzymatic catalyst (Figure S2b). Especially, the higher level of absorbance at 440 nm indicated the enhanced autoxidation and formation of bicyclic products in the presence of HRP (Figure 1e).<sup>43,44</sup>

The SC-HA conjugate with the gallol group possesses sufficient oxidative potential to initiate self-cross-linking and further accelerates the oxidative cross-linking process through self-production of oxidants. Although the polymer conjugates modified with other phenolic moieties (e.g., tyrosine, catechol) can also form the hydrogels via HRP-mediated cross-linking, oxidants like peroxide should be additionally supplemented to initiate oxidation reactions for cross-linking.<sup>45-47</sup> In contrast to the phenolic moieties with two hydroxyl groups, the gallol oxidation chemistry has an important unique feature: H<sub>2</sub>O<sub>2</sub> is produced as a byproduct during gallol autoxidation, and the generated peroxides serve as oxidants to accelerate the subsequent oxidation reaction of the unreacted gallol groups.<sup>40</sup> To observe this mechanistic role of the gallol group in SC-HA

hydrogel formation,  $\text{H}_2\text{O}_2$  generation during the incubation at room temperature was quantified. In this experiment, catechol-conjugated HA (CA-HA) (8.8% of catechol conjugation) with lower oxidative potential served as a control hydrogel system. As expected, the CA-HA conjugate generated a negligible amount of  $\text{H}_2\text{O}_2$  ( $0.6 \mu\text{M}$ ) during 24 h (Figure 1f). In contrast, the total generated  $\text{H}_2\text{O}_2$  in the SC-HA group was  $81.7 \mu\text{M}$ , which was significantly greater than the amount in the CA-HA group (Figure 1f). Interestingly, the addition of HRP to SC-HA increased  $\text{H}_2\text{O}_2$  production during the first 2 h, probably due to the HRP-mediated facilitation of the oxidation process. From 2 h onward,  $\text{H}_2\text{O}_2$  production in the SC-HA group with HRP was constantly lower ( $61.4 \mu\text{M}$  for 24 h) than that of the SC-HA group without HRP (Figure 1f), indicating that the generated  $\text{H}_2\text{O}_2$  was successively consumed by peroxidase for continuous autoxidation. Although the CA-HA conjugate is useful for injectable adhesive hydrogels, it mostly needs additional cross-linkers (e.g.,  $\text{Fe}^{3+}$  ions, sodium periodate, or HRP with  $\text{H}_2\text{O}_2$ ) for inducing oxidative cross-linking of the hydrogels. As shown in Figure 1f, CA-HA could not generate oxygen species capable of initiating self-cross-linking to form the HA hydrogel, while the SC-HA conjugate with gallol moieties could spontaneously generate  $\text{H}_2\text{O}_2$  due to its greater oxidative potential, thereby providing an in situ cross-linkable hydrogel system with no need of supplementary cross-linkers. Given that when  $\text{H}_2\text{O}_2$  generated by gallol autoxidation was consumed in the presence of peroxidase, dimerization of quinone intermediates of oxidized gallols was further promoted (Figures 1e,f, and S2), thus accelerating the cross-linking reactions to form the SC-HA hydrogel, gelation kinetics of the SC-HA hydrogel increased by autoxidation (Figure 1c,d) seems to be coordinated with the peroxidase-mediated coupling reaction.

The oxidation reaction by peroxidase to form the SC-HA hydrogel is highly biocompatible and also improves the mechanical property of the hydrogel. To evaluate the biocompatibility of the SC-HA hydrogel, HDFs were mixed with the SC-HA pregel solution (2%, w/v), and the cell-containing solution was cross-linked by treatment with HRP (0.06 and  $0.6 \text{ U mL}^{-1}$ ). Live/Dead cytotoxicity staining revealed that most of the encapsulated cells in the SC-HA hydrogel were viable after 1 and 7 days of in vitro culture, regardless of the HRP concentration [day 1:  $97.3 \pm 1.1\%$  ( $0.06 \text{ U mL}^{-1}$ ) and  $95.3 \pm 0.4\%$  ( $0.6 \text{ U mL}^{-1}$ ); day 7:  $94.5 \pm 1.0\%$  ( $0.06 \text{ U mL}^{-1}$ ) and  $92.3 \pm 1.4\%$  ( $0.6 \text{ U mL}^{-1}$ )] (Figures 1g,h and S3). Although  $\text{H}_2\text{O}_2$  produced during SC-HA gelation can reduce cellular metabolic activity at high concentrations, our SC-HA hydrogel system showed minimal cytotoxicity. This was probably due to the low amount of  $\text{H}_2\text{O}_2$  that was generated, which may not induce apoptotic cell death, and the continuous  $\text{H}_2\text{O}_2$  consumption needed for the autoxidation reaction.<sup>48</sup> SC-HA cross-linking upon the addition of HRP altered the mechanical properties of the resultant HA hydrogel. The SC-HA hydrogel formed in the presence of HRP exhibited a significantly higher elastic modulus ( $64.0 \pm 7.3 \text{ Pa}$ ) than the hydrogel formed without HRP ( $22.1 \pm 4.3 \text{ Pa}$ ) (Figure 1i). Moreover, the elasticity ( $\tan \delta = G''/G'$ ) was lower in SC-HA hydrogels formed with HRP than in hydrogels formed without HRP (SC-HA;  $0.41 \pm 0.06$  vs SC-HA/HRP;  $0.17 \pm 0.01$ ), indicating that elasticity was significantly increased by the addition of enzymes (Figure 1i). The improved mechanical property and elasticity are crucial for long-term stability of the injected hydrogel construct.<sup>23,49</sup> The collective observations

support the assumption that the self-cross-linking process of the SC-HA conjugate that is accelerated by inherent peroxidase in vivo after injection would be biocompatible and provide long-term stability of the filler construct with improved mechanical properties. Although the concentration and activity of peroxidase ( $0.06$  and  $0.6 \text{ U mL}^{-1}$ ) may not be identical to those of the in vivo environment (e.g.,  $0.44$  and  $1.32 \text{ U g}^{-1}$  glutathione peroxidase activity in human and mouse dermis tissues, respectively),<sup>50,51</sup> the HRP-mediated oxidative model could provide an effective in vitro system to recapitulate in vivo self-cross-linking of the SC-HA hydrogel. HRP addition was confirmed to accelerate oxidative cross-linking of SC-HA by promoting dimerization of oxidized gallols following self-production of oxygen species (Figures 1e,f, and S2), finally leading to faster gelation and improved mechanical properties of hydrogels (Figure 1c,d,i). Further rheometric investigation with a wider range of HRP activity ( $0.006$ ,  $0.06$ ,  $0.6$ , and  $6 \text{ U mL}^{-1}$ ), which may cover varied concentrations and activities of endogenous peroxidase in different tissues and in vivo situations, indicated that the elastic modulus and elasticity of the SC-HA hydrogel were gradually increased proportional to an increase in HRP activity up to  $6 \text{ U mL}^{-1}$  (Figure S4).

The SC-HA hydrogel possesses improved physical properties over previously reported tissue adhesive HA hydrogels such as the CA-HA hydrogel due to increased cross-linking density (Figure S5). During incubation of HA hydrogels under physiologically relevant conditions (in PBS at  $37 \text{ }^\circ\text{C}$ ), the weight of the CA-HA hydrogel increased more than 200% from its original state after 3 days and then further swelled up to 240% on day 7 of incubation, whereas the swelling level of SC-HA hydrogels was generally low (10–50%), which reached a plateau after 1 day of incubation. This result may indicate that the cross-linking density of the SC-HA hydrogel is greater than that of the CA-HA hydrogel. Oxidative gallol cross-linking seems to induce formation of more robust intermolecular polymeric networks in HA hydrogel constructs than the cross-linking reaction between oxidized catechol groups. Notably, the SC-HA hydrogel cross-linked via autoxidation without HRP addition showed a similar swelling ratio (48.2% on day 7 of incubation) to that of a previously reported gallol-modified HA hydrogel cross-linked by an oxidant ( $\text{NaIO}_4$ ).<sup>39</sup> With the increase of HRP concentration from  $0.06$  to  $0.6 \text{ U mL}^{-1}$ , a lower swelling of the SC-HA hydrogel was observed, indicating increased cross-linking density of the hydrogels proportional to enzymatic activity for oxidation.

Next, we evaluated the injectability of the SC-HA filler using different-sized needles. The injection force of the dermal filler is affected by rheological and physiochemical properties of the filler composite, which include viscosity, particle size, cross-linking density, and polymer concentration.<sup>20</sup> In particular, the use of conventional dermal fillers containing large particulates ( $>400 \mu\text{m}$ ) or having high viscosity for stable deep-tissue applications usually requires large needles (23–27 G); otherwise, high pressure during injection is inevitable.<sup>49</sup> High pressure during injection is undesirable, since it may push small vessels or nerves near the injection site, resulting in devastating complications associated with vascular damage and nerve block.<sup>52</sup> In addition, the larger perforation by large needles increases the frequency of pain, bleeding, and subsequent infection.<sup>53,54</sup> Therefore, dermal filler should be injectable without high pressure, even when small-gauge needles are used, to avoid pain and potential complications.

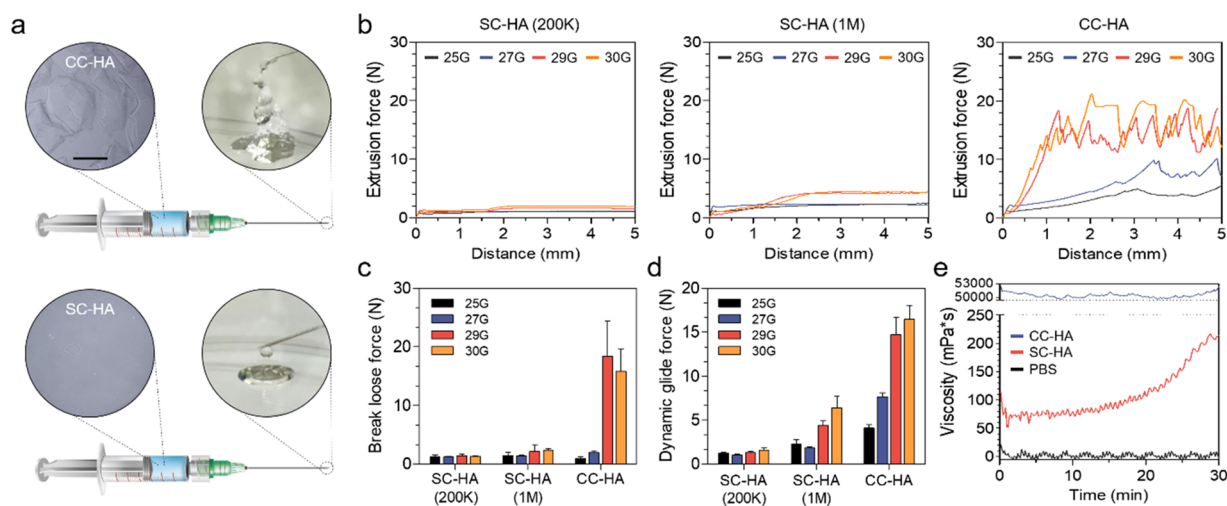


**Figure 2.** Injectability of SC-HA hydrogel fillers. (a) Microscopic and macroscopic views of CC-HA filler (upper) and SC-HA filler (lower) composites. (b) Profiles of extrusion force of CC-HA and SC-HA (200 K, 1 M) fillers in various-sized needles (25, 27, 29, 30 G). (c) Break loose force (the force needed to initiate the movement of plunger) and (d) dynamic glide force (the force needed to sustain the movement of plunger). CC-HA filler and SC-HA fillers (200 K, 1 M) were tested with different gauge needles ( $n = 4$ ). (e) Viscosities of PBS, CC-HA filler, and SC-HA hydrogel solution as a function of time.

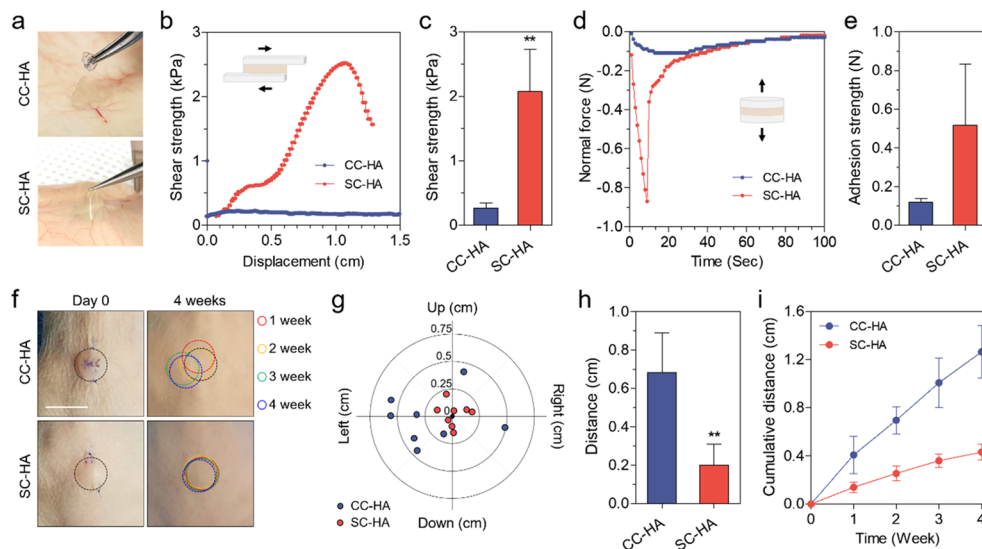


**Figure 3.** Tissue adhesion and displacement of SC-HA fillers. (a) Adhesion of the CC-HA filler and the SC-HA hydrogel filler on the skin tissue after 1 month of injection into the subcutaneous regions of mice. (b) Lap shear test for comparing shear strength of the CC-HA filler and the SC-HA hydrogel filler placed between mouse skin tissues and (c) average maximum shear strength of each filler composite ( $n = 3$ , \*\*,  $p < 0.01$ , compared to the CC-HA group). (d) Tack test to measure the detachment force of the CC-HA filler and the SC-HA hydrogel filler placed between mouse skin tissues and (e) average adhesion strength of each filler composite ( $n = 3$ ). For in vitro formation of SC-HA hydrogel,  $0.06 \text{ U mL}^{-1}$  HRP was added to a 2% (w/v) SC-HA pregel solution. (f) Displacement of the CC-HA filler and the SC-HA hydrogel filler during the 4 weeks after subcutaneous injection. (g) Diagram demonstrating the location of each filler construct displaced from the initial site (center of the diagram) and (h) average distance from the initial site 4 weeks after the injection ( $n = 8$ , \*\*,  $p < 0.01$ , compared to the CC-HA group). (i) Cumulative displacement distance during 4 weeks after the injection ( $n = 8$ ).

A commercially available and representative biphasic, chemically cross-linked HA (CC-HA) filler product (Restylane), which is cross-linked by BDDE without HRP, was used as a control for the comparison of filler injectability. Inhomogeneous HA particulates (400–1000  $\mu\text{m}$  in size) were observed within the CC-HA filler, while there were no aggregated constructs in the SC-HA filler solution (Figure 2a). To measure the force during injection with a universal testing machine, each filler composite was loaded in a 1 mL syringe and pressed with an injection speed of  $12.5 \text{ mm s}^{-1}$  using 25, 27, 29, and 30 G needles. In the SC-HA group, viscous

liquidlike composites could be smoothly injected, regardless of the molecular weight of HA (200 kDa and 1 MDa). There was a slight increase in the extrusion force when smaller needles (29 and 30 G) were tested for the injection of the 1 M SC-HA filler (Figure 2b). However, the CC-HA filler composite required a much larger injection force than the SC-HA filler because the size of the particle-based filler composite exceeded the inner diameter of needles ( $<400 \mu\text{m}$ ) (Figure 2b). In addition, we measured the break loose force (Figure 2c) and dynamic glide force (Figure 2d), which is the force needed to initiate the movement of the plunger and the force required to

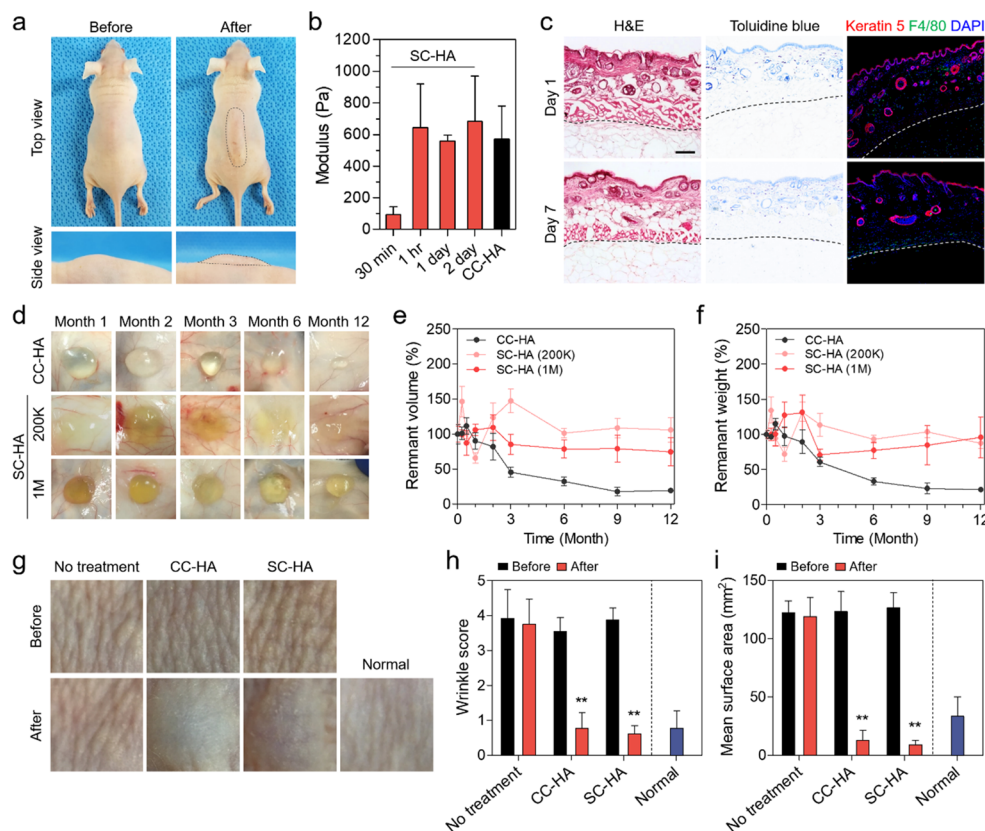


**Figure 4.** In vivo application of SC-HA fillers for safe, long-lasting volumetric tissue augmentation and wrinkle correction. (a) Gross view of the tissue volume before and after SC-HA filler injection. Dashed line indicates newly augmented tissue by SC-HA hydrogel filler injection. (b) Elastic modulus (at 1 Hz) of SC-HA filler composite retrieved at predetermined time points after subcutaneous injection ( $n = 3$ ). CC-HA filler composite retrieved after 2 days was used as a control. (c) Histological analysis with H&E, toluidine blue, and immunofluorescence (keratin 5, red; F4/80, green; nuclei, blue) staining of SC-HA fillers adjacent to skin tissues 1 and 7 days after subcutaneous injection. Dashed lines indicate the boundary between tissues and the injected filler composites. Scale bar is  $200 \mu\text{m}$ . (d) CC-HA filler composites and SC-HA fillers (200 K, 1 M) retrieved at predetermined time points up to 12 months after injection into subcutaneous space of mice. (e) Volume and (f) weight of the remaining filler constructs harvested at each time point ( $n = 4-8$ ). (g) Gross view of wrinkles on mouse skin before and after tissue augmentation by HA filler injection. Control group is a normal mouse skin without wrinkle induction. (h) Scoring evaluation and (i) mean surface area of wrinkles before and after SC-HA and CC-HA filler injection ( $n = 6-8$ , \*\*,  $p < 0.01$ , compared to before the injection of each filler).

sustain the movement of the plunger, respectively. Both the 200 K and 1 M SC-HA fillers exhibited a low break loose force with all of the needles. However, the CC-HA filler required a significantly larger break loose force, especially when small-gauge needles (29 and 30 G) were used for injection (Figure 2c). The SC-HA filler with the 200 K HA backbone had a constantly low dynamic glide force irrespective of the needle size (Figure 2d). Although the SC-HA filler with a larger molecular weight (1 M) needed a somewhat higher dynamic glide force as the needle size decreased (29 and 30 G), the CC-HA filler required a significantly larger dynamic glide force, compared with the SC-HA filler (Figure 2d). We also found that the viscosity of SC-HA dissolved in PBS gradually increased due to cross-linking by autoxidation in the ambient air condition, but the value (50–200 mPa s) was significantly lower than that of the CC-HA filler with a viscosity over 50 000 mPa s (Figure 2e). From these results, we could conclude that the dermal injectability of SC-HA fillers is superior to that of CC-HA fillers, which significantly reduces pain, bleeding, and tissue damage in clinical situations.

In addition to their poor injectability, a critical limitation of commercial biphasic CC-HA fillers is that filler displacement often occurs from the original injected site by external force, gravity, and daily muscular movement. The migration of the

injected filler constructs or their parts to unwanted positions may produce complications, such as inflammation at a location distal from the injected site, which requires additional and complicated processes including repositioning, reinjection, and even removal of the constructs in emergent situations.<sup>55,56</sup>

Given the robust affinity of oxidized gallol moieties to various proteins, the gallol-modified hydrogels could exhibit excellent tissue adhesion, even when wet.<sup>37-39</sup> We have previously demonstrated that formation of various quinone intermediates and bicyclic products during oxidation of gallol groups enables strong adhesion of the gallol-modified hydrogel to a tissue surface.<sup>39</sup> Indeed, when the filler composites were harvested with adherent skin tissues 1 month after injection into subcutaneous spaces of mice, the SC-HA fillers tightly adhered to the skin tissue, while commercial CC-HA fillers weakly interacted with surrounding skin tissues and barely attached to the tissue (Figure 3a). To measure the adhesion strength, SC-HA pregel solution [2% (w/v) in PBS] supplemented with HRP ( $0.06 \text{ U mL}^{-1}$ ) was placed between mouse skin tissues anchored on glass slides and then fully cross-linked for 3 h in a humidified chamber. The subsequent lap shear test revealed that the shear strength of the SC-HA filler ( $2.07 \pm 0.66 \text{ kPa}$ ) was 7.6-fold greater than that of the CC-HA filler ( $0.27 \pm 0.08 \text{ kPa}$ ), indicating that the SC-HA filler was more resistant to

displacement than the commercial CC-HA filler (Figure 3b,c). The detachment stress of HA fillers from mouse skin tissue was also measured using a rheometer in the tack test mode. The adhesion strength was higher in the SC-HA filler group ( $0.51 \pm 0.32$  N) than in the CC-HA filler group ( $0.12 \pm 0.01$  N) (Figure 3d,e), consistent with the lap shear test result.

The excellent tissue adhesive property of the SC-HA hydrogel would allow for the stable and long-term retention in vivo of the injected HA filler, which cannot be achieved with conventional CC-HA filler systems. The fixability of the SC-HA filler was further evaluated by monitoring the movement of the injected filler constructs in subcutaneous spaces of mice. Four weeks after injection, most of the CC-HA filler constructs were displaced from where they were first injected, but the SC-HA fillers remained around the injection site (Figure 3f). The final distance from the initial position of the injected filler composite indicated that displacement was significantly prevented in the SC-HA filler group compared with that in the CC-HA filler group (CC-HA:  $0.68 \pm 0.2$  cm; SC-HA:  $0.2 \pm 0.11$  cm) (Figure 3g,h). The cumulative migration distance during the 4 weeks of observation also demonstrated the retention of SC-HA fillers at the desired position in contrast to CC-HA fillers (Figure 3i). Based on its excellent tissue adhesiveness, the SC-HA hydrogel filler could be stably maintained at the original injection site with minimal migration.

Finally, the cosmetic application of the SC-HA hydrogel filler was demonstrated for volumetric tissue augmentation and wrinkle correction. The SC-HA pregel solution at 2% (w/v) concentration was injected using a 30 G syringe into subcutaneous regions of mice. The injected SC-HA pregel solution devoid of cross-linking agents formed three-dimensional hydrogel filler constructs via autoxidation in vivo approximately 10 min after injection. The shape of the SC-HA filler could be easily adjusted before the formation of a fully cross-linked hydrogel, and volumetric augmentation was clearly observed at the injected site (Figure 4a). The in vivo cross-linking to form robust SC-HA hydrogel fillers was confirmed by measuring the mechanical property of the HA filler constructs retrieved at several time points after injection into the subcutaneous space (Figure 4b). Interestingly, the elastic modulus ( $G'$ ) of the SC-HA hydrogel filler (200 kDa HA) 30 min after injection (93.7 Pa) was higher than that of the SC-HA hydrogel prepared via in vitro oxidative cross-linking by HRP (64.0 Pa). The  $G'$  of the SC-HA hydrogel further increased to 644.7 Pa 1 h after injection and remained at similar levels for the next 2 days. Although the SC-HA filler was injected as a viscous solution without any cross-linking agents, gallol oxidation mediated by endogenous enzymes (e.g., peroxidases) that were abundant in subcutaneous tissue induced in vivo cross-linking of SC-HA, successfully generating stable and robust hydrogel constructs with comparable mechanical properties to conventional biphasic CC-HA filler composites (Figure 4b). To evaluate inflammation by the SC-HA filler, injected SC-HA hydrogels attached to surrounding tissues were stained using H&E and toluidine blue (Figure 4c). These histological analyses revealed that the injection and in vivo cross-linking of the SC-HA hydrogel did not trigger any significant infiltration of inflammatory cells within or around the hydrogel constructs 1 and 7 days after the injection, indicating the excellent biocompatibility of the SC-HA filler. The immunostaining against F4/80 revealed that few macrophages were detected within or around the SC-HA hydrogel

filler constructs 1 and 7 days after injection into the subcutaneous space of mouse (Figure 4c), which indicates that injection of the SC-HA hydrogel did not evoke any significant inflammation, confirming the biocompatibility of the SC-HA filler again.

Most importantly, the SC-HA hydrogel showed excellent performance as an injectable dermal filler for tissue augmentation, wrinkle correction, and long-term volumetric maintenance. Longevity of the injected filler is another important requirement for patients to minimize cost and retain the long-term effect of the filler. To evaluate the in vivo retention of HA fillers, SC-HA fillers (200 K and 1 M) and CC-HA filler composites (1 M) were subcutaneously injected and retrieved at several time points up to 1 year to examine physiochemical changes in volume and weight of the constructs. In the CC-HA filler group, the constructs gradually degraded, and only about 50% of the initial volume and weight remained 3 months after injection, and nearly 80% of the injected filler was eliminated 1 year after injection (Figure 4d–f). However, our SC-HA filler constructs were well maintained without significant reduction in volume and weight for 1 year, regardless of molecular weight, demonstrating the potential of the SC-HA hydrogel as a safe, long-term stable injectable filler for volumetric augmentation (Figure 4d–f). The functionality of the SC-HA filler for wrinkle correction was assessed in a mouse model of wrinkles. Formation of wrinkles in mouse skin was chemically induced by treatment with calcitriol solution for 6 weeks.<sup>29</sup> Injection of the SC-HA filler under the wrinkled skin tissue resulted in tissue augmentation and wrinkle correction (Figure 4g). The surface morphology of the wrinkled skin tissue was visualized using a skin visiometer. The replica image revealed that the SC-HA filler clearly reduced wrinkles on mouse skin (Figure 6Sa). All of the dimensional indexes demonstrating the level of wrinkles, including total wrinkle area, total wrinkle length, mean wrinkle length, and mean wrinkle depth, were significantly decreased after injecting the SC-HA filler, indicating successful volumetric augmentation and wrinkle correction (Figure 6Sb). For scoring evaluation, the degree of wrinkle was ranged from 0 to 5 following the evaluation criteria described by Lemperle et al.<sup>42</sup> When HA hydrogel fillers were injected under the skin tissue with chemically induced wrinkles, both CC-HA and SC-HA fillers significantly reduced wrinkles on the skin. The scores of corrected wrinkles by those HA fillers were of similar levels to that of normal mouse skin without wrinkle induction (Figure 4h). The mean surface area of wrinkle was also significantly reduced after injecting both types of HA fillers, indicating that the wrinkle correction by SC-HA fillers is comparable to that by commercial CC-HA fillers (Figure 4i).

In addition, based on the higher binding affinity of the oxidized gallol moiety to nucleophiles in proteins, SC-HA can provide a functional dermal filler that delivers growth factors to enhance skin tissue regeneration in a sustained and controlled manner. Our previous studies demonstrated that catechol- or gallol-functionalized hydrogels can retain the encapsulated proteins for a long time due to their ability to tether the proteins.<sup>39,57</sup> Thus, growth factor-containing SC-HA fillers could allow the sustained release of proteins in vivo from the gradually degraded HA hydrogel. The ELISA data showing the release profiles of EGF during incubation under physiologically relevant conditions (in PBS at 37 °C) revealed that only a small amount of EGF (~10% of the initially loaded EGF) was



released from SC-HA hydrogel fillers in the absence of hyaluronidase due to a great avidity of oxidized gallol groups to proteins, but EGF was gradually released from SC-HA filler constructs upon hyaluronidase treatment (Figure S7a). This result may indicate that growth factors for skin regeneration could be sustainably released from SC-HA hydrogel fillers in vivo over a long-term period, speculating the regenerative potential of the growth factor-incorporated SC-HA hydrogel as a functional dermal filler. We injected the SC-HA pregel solution including EGF (10  $\mu\text{g}$  dose) under a mouse skin with chemically induced wrinkles. After 1 month of the injection, H&E staining revealed that the SC-HA filler containing EGF produced dermal histological morphology similar to that of normal wrinkle-free skin (Figure S7b). Masson's trichrome staining indicated that collagen deposition in the dermis was increased in the SC-HA filler group with EGF compared with the untreated group (Figure S7b). These results suggest the possibility of an injectable SC-HA hydrogel as a functional dermal filler that corrects wrinkles and promotes skin regeneration.

The SC-HA hydrogel developed herein has several novel aspects and advantages over previously reported gallol-modified hydrogels. The main idea of this study is to apply gallol chemistry for a cross-linker-free injectable hydrogel filler that is highly biocompatible and long-term stable with minimal displacement. Several studies including ours demonstrated gallol-conjugated polymers and their oxidative cross-linking to form hydrogels with tissue adhesive properties. Hydrogel formation in our current study and those previous studies was basically mediated via the same type of reaction (oxidation of gallols conjugated to the polymer backbone), but gallol oxidation was induced by different cross-linking processes. Most previous studies relied on supplementary chemical agents (e.g., oxidants, ions) for oxidative gallol cross-linking reactions.<sup>38,39,58,59</sup> Gallol oxidation by additional cross-linkers is highly efficient but sometimes induces too rapid gelation, which impairs the injectability of hydrogels and hinders uniform distribution of intermolecular polymer networks in the hydrogel constructs. Thus, in the present study, we employed a different chemical cross-linking mode by  $\text{H}_2\text{O}_2$  generated by autoxidation of gallols even in the absence of exogenous cross-linkers, suggesting an in situ self-cross-linkable hydrogel model. Due to self-production of oxygen species of oxidized gallols and endogenous peroxidase-mediated coupling reaction under in vivo conditions, we could demonstrate easily injectable HA hydrogel filler systems without any additional cross-linkers. In contrast to previously reported gallol-conjugated polymers incorporated with cross-linkers, since the SC-HA conjugate can be injected in a solution state with low viscosity, it is readily injectable even when using small-gauge syringe needles, thus allowing significant reduction in pain, bleeding, and tissue damage, which is hardly accomplished with conventional gallol-conjugated hydrogels due to rapid gelation initiated by cross-linkers before injection. Although the final chemical adducts by gallol oxidation reaction may be almost identical in our current study and previous studies, different mediators are involved in the cross-linking process, allowing us to adjust gelation kinetics that is more feasible for injectable hydrogel filler application. Since there is no need of cross-linkers, this can also remove potential safety issues caused by additional chemical cross-linkers.

More importantly, remarkably improved long-term in vivo stability of SC-HA hydrogel fillers may be attributed to the

absence of supplementary cross-linkers such as oxidants. It has been known that reactive oxygen species and hydroxyl radicals can induce oxidative degradation of HA by mediating sugar ring opening in the HA backbone.<sup>60,61</sup> Degradation of the HA backbone is also known to generate  $\text{H}_2\text{O}_2$  as a byproduct,<sup>62</sup> which further accelerates oxidative opening of the HA sugar ring. Consequently, oxidants (e.g.,  $\text{NaIO}_4$ ) used to cross-link gallol-modified HA may affect the degradation profiles of hydrogels.<sup>39</sup> As SC-HA in our current study does not require the addition of such oxidants for gelation, the levels of reactive oxygen species and radicals in SC-HA hydrogels are assumed to be lower than those in gallol-modified HA hydrogels cross-linked by exogenously added oxidants. Although  $\text{H}_2\text{O}_2$  is generated from autoxidation of gallols in SC-HA, it is most likely to be consumed by innate peroxidase in tissues and then used for a series of oxidative reactions for cross-linking rather than for HA degradation. Therefore, in vivo cross-linking of SC-HA via gallol autoxidation alone without exogenous oxidants could minimize degradation of the HA backbone during the gelation process, contributing to the improved long-term stability of SC-HA hydrogel filler constructs in vivo. Under inflammatory conditions with an increased level and activity of reactive oxygen species and radicals, it should be more critical to minimize oxidative degradation of HA for long-term maintenance. Previous studies demonstrated that chemicals (e.g., captopril, tiopronin) and enzymes (e.g., catalase) possessing radical scavenging activity prevent HA oxidative degradation.<sup>60,62</sup> A combination strategy with radical scavenging molecules could expand the application of SC-HA hydrogels to injured tissues with severe inflammation.

Lastly, we demonstrate the potential of the SC-HA hydrogel as a functional dermal filler capable of mediating sustained and controlled drug delivery for tissue regeneration (Figure S7). Overall, the concept of in situ chemical cross-linking through coordination of gallol autoxidation and endogenous oxidative enzymatic reaction may be able to provide novel chemical aspects of our SC-HA hydrogel system and facilitate development of multifunctional biomaterials controllable in a more sophisticated manner and highly feasible for human translational approach.

## CONCLUSIONS

The findings demonstrate the applicability of the gallol-modified HA hydrogel as a self-cross-linkable filler with no need of cross-linking agents or catalysts for cosmetic and plastic reconstruction. The performance of our SC-HA hydrogel as an injectable dermal filler was superior to that of commercially available, chemically cross-linked biphasic HA filler composites in terms of injectability, tissue adhesiveness, and long-term volumetric augmentation. The SC-HA filler could be smoothly injected even using small-gauge syringe needles. The improved tissue adhesive ability and mechanical stability of the SC-HA filler allowed for long-term retention of the filler constructs at the original injection sites without adverse effects. The potential mechanism of the in vivo self-cross-linking of the SC-HA hydrogel filler may be involved in  $\text{H}_2\text{O}_2$  self-production from oxidized SC-HA and a series of oxidative reactions facilitated by innate peroxidases in the tissue. Our novel strategy based on a self-cross-linked hydrogel overcomes the limitations of the current cross-linking methods for HA-based fillers and provides a highly biocompatible, easily injectable, and mechanically stable filler system. The catalyst-free strategy exploited in this study could be further expanded

to diverse biomedical applications, including cell therapy, tissue engineering, and drug delivery, by incorporating functional cells or specific drugs.

## ■ ASSOCIATED CONTENT

### Supporting Information

The Supporting Information is available free of charge at <https://pubs.acs.org/doi/10.1021/acs.chemmater.9b02802>.

<sup>1</sup>H NMR analysis, UV–vis spectroscopy analysis, in vitro biocompatibility test, rheological analysis, swelling test, evaluation of wrinkle correction, and functional evaluation of SC-HA fillers supplemented with EGF (PDF)

## ■ AUTHOR INFORMATION

### Corresponding Author

\*E-mail: [seungwoocho@yonsei.ac.kr](mailto:seungwoocho@yonsei.ac.kr).

### ORCID

Seung-Woo Cho: 0000-0001-8058-332X

### Author Contributions

<sup>†</sup>J.S.L. and J.H.C. contributed equally to this work.

### Author Contributions

The manuscript was written through contribution of all authors. All authors have given approval to the final version of the manuscript.

### Notes

The authors declare no competing financial interest.

## ■ ACKNOWLEDGMENTS

The protocol for animal experiments was reviewed and approved by the Institutional Animal Care and Use Committee (IACUC) of the Yonsei Laboratory Animal Research Center (YLARC) (protocol number: IACUC-201802-700-01). This work was supported by grants (2017R1A2B3005994 and 2018M3A9H1021382) from the National Research Foundation (NRF) of Korea funded by the Ministry of Science and ICT (MSIT), Republic of Korea. This work was also supported by the Institute for Basic Science (IBS-R026-D1).

## ■ REFERENCES

- (1) Gaharwar, A. K.; Peppas, N. A.; Khademhosseini, A. Nano-composite hydrogels for biomedical applications. *Biotechnol. Bioeng.* **2014**, *111*, 441–453.
- (2) Hoffman, A. S. Hydrogels for biomedical applications. *Adv. Drug Delivery Rev.* **2012**, *64*, 18–23.
- (3) Burdick, J. A.; Prestwich, G. D. Hyaluronic acid hydrogels for biomedical applications. *Adv. Mater.* **2011**, *23*, H41–H56.
- (4) Li, Y.; Rodrigues, J.; Tomás, H. Injectable and biodegradable hydrogels: gelation, biodegradation and biomedical applications. *Chem. Soc. Rev.* **2012**, *41*, 2193–2221.
- (5) Kim, E. H.; Lim, S.; Kim, T. E.; Jeon, I. O.; Choi, Y. S. Preparation of in situ injectable chitosan/gelatin hydrogel using an acid-tolerant tyrosinase. *Biotechnol. Bioprocess Eng.* **2018**, *23*, 500–506.
- (6) Lee, J. H. Injectable hydrogels delivering therapeutic agents for disease treatment and tissue engineering. *Biomater. Res.* **2018**, *22*, No. 27.
- (7) Varma, D. M.; Gold, G. T.; Taub, P. J.; Nicoll, S. B. Injectable carboxymethylcellulose hydrogels for soft tissue filler applications. *Acta Biomater.* **2014**, *10*, 4996–5004.
- (8) Bellas, E.; Lo, T. J.; Fournier, E. P.; Brown, J. E.; Abbott, R. D.; Gil, E. S.; Marra, K. G.; Rubin, J. P.; Leisk, G. G.; Kaplan, D. L. Injectable silk foams for soft tissue regeneration. *Adv. Healthcare Mater.* **2015**, *4*, 452–459.

- (9) Shuck, J.; Iorio, M. L.; Hung, R.; Davison, S. P. Autologous fat grafting and injectable dermal fillers for human immunodeficiency virus-associated facial lipodystrophy: a comparison of safety, efficacy, and long-term treatment outcomes. *Plast. Reconstr. Surg.* **2013**, *131*, 499–506.

- (10) Jagdeo, J.; Ho, D.; Lo, A.; Carruthers, A. A systematic review of filler agents for aesthetic treatment of HIV facial lipoatrophy (FLA). *J. Am. Acad. Dermatol.* **2015**, *73*, 1040.e14–1054.e14.

- (11) Carruthers, A.; Carruthers, J. Evaluation of injectable calcium hydroxylapatite for the treatment of facial lipoatrophy associated with human immunodeficiency virus. *Dermatol. Surg.* **2008**, *34*, 1486–1499.

- (12) Gamboa-Bobadilla, G. M. Implant breast reconstruction using acellular dermal matrix. *Ann. Plast. Surg.* **2006**, *56*, 22–25.

- (13) Bigatà, X.; Ribera, M.; Bielsa, I.; Ferrándiz, C. Adverse granulomatous reaction after cosmetic dermal silicone injection. *Dermatol. Surg.* **2001**, *27*, 198–200.

- (14) Lemperle, G.; Morhenn, V.; Charrier, U. Human histology and persistence of various injectable filler substances for soft tissue augmentation. *Aesthetic Plast. Surg.* **2003**, *27*, 354–366.

- (15) Requena, L.; Requena, C.; Christensen, L.; Zimmermann, U. S.; Kutzner, H.; Cerroni, L. Adverse reactions to injectable soft tissue fillers. *J. Am. Acad. Dermatol.* **2011**, *64*, 1–34.

- (16) Skrzypek, E.; Górnicka, B.; Skrzypek, D. M.; Krzysztof, M. R. Granuloma as a complication of polycaprolactone-based dermal filler injection: ultrasound and histopathology studies. *J. Cosmet. Laser Ther.* **2019**, *21*, 65–68.

- (17) Alijotas-Reig, J.; Fernández-Figueras, M. T.; Puig, L. Late-onset inflammatory adverse reactions related to soft tissue filler injections. *Clin. Rev. Allergy Immunol.* **2013**, *45*, 97–108.

- (18) Cho, K.-H.; Uthaman, S.; Park, I.-K.; Cho, C.-S. Injectable biomaterials in plastic and reconstructive surgery: a review of the current status. *Tissue Eng. Regen. Med.* **2018**, *15*, 559–574.

- (19) Fakhari, A.; Berkland, C. Applications and emerging trends of hyaluronic acid in tissue engineering, as a dermal filler and in osteoarthritis treatment. *Acta Biomater.* **2013**, *9*, 7081–7092.

- (20) Tezel, A.; Fredrickson, G. H. The science of hyaluronic acid dermal fillers. *J. Cosmet. Laser Ther.* **2008**, *10*, 35–42.

- (21) Zamboni, F.; Vieira, S.; Reis, R. L.; Oliveira, J. M.; Collins, M. N. The potential of hyaluronic acid in immunoprotection and immunomodulation: chemistry, processing and function. *Prog. Mater. Sci.* **2018**, *97*, 97–122.

- (22) Micheels, P.; Besse, S.; Flynn, T. C.; Sarazin, D.; Elbaz, Y. Superficial dermal injection of hyaluronic acid soft tissue fillers: comparative ultrasound study. *Dermatol. Surg.* **2012**, *38*, 1162–1169.

- (23) Edsman, K.; Nord, L. I.; Öhrlund, Å.; Lärkner, H.; Kenne, A. H. Gel properties of hyaluronic acid dermal fillers. *Dermatol. Surg.* **2012**, *38*, 1170–1179.

- (24) Chun, C.; Lee, D. Y.; Kim, J.-T.; Kwon, M.-K.; Kim, Y.-Z.; Kim, S.-S. Effect of molecular weight of hyaluronic acid (HA) on viscoelasticity and particle texturing feel of HA dermal biphasic fillers. *Biomater. Res.* **2016**, *20*, No. 24.

- (25) Pierre, S.; Liew, S.; Bernardin, A. Basics of dermal filler rheology. *Dermatol. Surg.* **2015**, *41*, S120–S126.

- (26) Ducher, G.; Prasetyo, A. D.; Rubin, M. G.; Moretti, E. A.; Nikolis, A.; Prager, W. Hyaluronic acid fillers with cohesive polydensified matrix for soft-tissue augmentation and rejuvenation: a literature review. *Clin., Cosmet. Invest. Dermatol.* **2016**, *9*, 257–280.

- (27) Edsman, K.; Öhrlund, Å. Cohesion of hyaluronic acid fillers: correlation between cohesion and other physicochemical properties. *Dermatol. Surg.* **2018**, *44*, 557–562.

- (28) Tran, C.; Carraux, P.; Micheels, P.; Kaya, G.; Salomon, D. In vivo bio-integration of three hyaluronic acid fillers in human skin: a histological study. *Dermatology* **2014**, *228*, 47–54.

- (29) Yeom, J.; Bhang, S. H.; Kim, B.-S.; Seo, M. S.; Hwang, E. J.; Cho, I. H.; Park, J. K.; Hahn, S. K. Effect of cross-linking reagents for hyaluronic acid hydrogel dermal fillers on tissue augmentation and regeneration. *Bioconjugate Chem.* **2010**, *21*, 240–247.

- (30) De Boule, K.; Glogau, R.; Kono, T.; Nathan, M.; Tezel, A.; Roca-Martinez, J.-X.; Paliwal, S.; Stroumpoulis, D. A review of the metabolism of 1, 4-butanediol diglycidyl ether-crosslinked hyaluronic acid dermal fillers. *Dermatol. Surg.* **2013**, *39*, 1758–1766.
- (31) Ryu, J. H.; Lee, Y.; Kong, W. H.; Kim, T. G.; Park, T. G.; Lee, H. Catechol-functionalized chitosan/pluronic hydrogels for tissue adhesives and hemostatic materials. *Biomacromolecules* **2011**, *12*, 2653–2659.
- (32) Shin, J.; Lee, J. S.; Lee, C.; Park, H. J.; Yang, K.; Jin, Y.; Ryu, J. H.; Hong, K. S.; Moon, S. H.; Chung, H. M. Tissue adhesive catechol-modified hyaluronic acid hydrogel for effective, minimally invasive cell therapy. *Adv. Funct. Mater.* **2015**, *25*, 3814–3824.
- (33) Lee, B. P.; Dalsin, J. L.; Messersmith, P. B. Synthesis and gelation of DOPA-modified poly (ethylene glycol) hydrogels. *Biomacromolecules* **2002**, *3*, 1038–1047.
- (34) Lee, Y.; Chung, H. J.; Yeo, S.; Ahn, C.-H.; Lee, H.; Messersmith, P. B.; Park, T. G. Thermo-sensitive, injectable, and tissue adhesive sol-gel transition hyaluronic acid/pluronic composite hydrogels prepared from bio-inspired catechol-thiol reaction. *Soft Matter* **2010**, *6*, 977–983.
- (35) Barrett, D. G.; Fullenkamp, D. E.; He, L.; Holten-Andersen, N.; Lee, K. Y. C.; Messersmith, P. B. pH-based regulation of hydrogel mechanical properties through mussel-inspired chemistry and processing. *Adv. Funct. Mater.* **2013**, *23*, 1111–1119.
- (36) Shin, M.; Lee, H. Gallol-rich hyaluronic acid hydrogels: shear-thinning, protein accumulation against concentration gradients, and degradation-resistant properties. *Chem. Mater.* **2017**, *29*, 8211–8220.
- (37) Zhan, K.; Kim, C.; Sung, K.; Ejima, H.; Yoshie, N. Tunicate-inspired gallol polymers for underwater adhesive: a comparative study of catechol and gallol. *Biomacromolecules* **2017**, *18*, 2959–2966.
- (38) Oh, D. X.; Kim, S.; Lee, D.; Hwang, D. S. Tunicate-mimetic nanofibrous hydrogel adhesive with improved wet adhesion. *Acta Biomater.* **2015**, *20*, 104–112.
- (39) Cho, J. H.; Lee, J. S.; Shin, J.; Jeon, E. J.; An, S.; Choi, Y. S.; Cho, S. W. Ascidian-inspired fast-forming hydrogel system for versatile biomedical applications: pyrogallol chemistry for dual modes of crosslinking mechanism. *Adv. Funct. Mater.* **2018**, *28*, No. 1705244.
- (40) Lee, F.; Chung, J. E.; Xu, K.; Kurisawa, M. Injectable degradation-resistant hyaluronic acid hydrogels cross-linked via the oxidative coupling of green tea catechin. *ACS Macro Lett.* **2015**, *4*, 957–960.
- (41) Collins, M. N.; Birkinshaw, C. Hyaluronic acid solutions—a processing method for efficient chemical modification. *J. Appl. Polym. Sci.* **2013**, *130*, 145–152.
- (42) Lemperle, G.; Holmes, R. E.; Cohen, S. R.; Lemperle, S. M. A classification of facial wrinkles. *Plast. Reconstr. Surg.* **2015**, *108*, 1735–1750.
- (43) Aronson, S.; Roof, R. B., Jr.; Belle, J. Kinetic study of the oxidation of uranium dioxide. *J. Chem. Phys.* **1957**, *27*, 137–144.
- (44) Shin, M.; Galarraga, J. H.; Kwon, M. Y.; Lee, H.; Burdick, J. A. Gallol-derived ECM-mimetic adhesive bioinks exhibiting temporal shear-thinning and stabilization behavior. *Acta Biomater.* **2019**, *95*, 165–175.
- (45) Teixeira, L. S. M.; Feijen, J.; van Blitterswijk, C. A.; Dijkstra, P. J.; Karperien, M. Enzyme-catalyzed crosslinkable hydrogels: emerging strategies for tissue engineering. *Biomaterials* **2012**, *33*, 1281–1290.
- (46) Hou, J.; Li, C.; Guan, Y.; Zhang, Y.; Zhu, X. X. Enzymatically crosslinked alginate hydrogels with improved adhesion properties. *Polym. Chem.* **2015**, *6*, 2204–2213.
- (47) Roberts, J. J.; Naudiyal, P.; Lim, K. S.; Poole-Warren, L. A.; Martens, P. J. A comparative study of enzyme initiators for crosslinking phenol-functionalized hydrogels for cell encapsulation. *Biomater. Res.* **2016**, *20*, No. 30.
- (48) Asada, S.; Fukuda, K.; Oh, M.; Hamanishi, C.; Tanaka, S. Effect of hydrogen peroxide on the metabolism of articular chondrocytes. *Inflamm. Res.* **1999**, *48*, 399–403.
- (49) Kablik, J.; Monheit, G.; Yu, L.; Chang, G.; Gershkovich, J. Comparative physical properties of hyaluronic acid dermal fillers. *Dermatol. Surg.* **2009**, *35*, 302–312.
- (50) Shindo, Y.; Witt, E.; Han, D.; Epstein, W.; Packer, L. Enzymic and non-enzymic antioxidants in epidermis and dermis of human skin. *J. Invest. Dermatol.* **1994**, *102*, 122–124.
- (51) Shindo, Y.; Witt, E.; Packer, L. Antioxidant defense mechanisms in murine epidermis and dermis and their responses to ultraviolet light. *J. Invest. Dermatol.* **1993**, *100*, 260–265.
- (52) Owczarz, M.; Bolisetty, S.; Mezzenga, R.; Arosio, P. Sol-gel transition of charged fibrils composed of a model amphiphilic peptide. *J. Colloid Interface Sci.* **2015**, *437*, 244–251.
- (53) Gill, H. S.; Prausnitz, M. R. Does needle size matter? *J. Diabetes Sci. Technol.* **2007**, *1*, 725–729.
- (54) Lim, A. C. Hyaluronic acid filler injections with a 31-gauge insulin syringe. *Australas. J. Dermatol.* **2010**, *51*, 74–75.
- (55) Chae, S. Y.; Lee, K. C.; Jang, Y. H.; Lee, S. J.; Kim, D. W.; Lee, W. J. A case of the migration of hyaluronic acid filler from nose to forehead occurring as two sequential soft lumps. *Ann. Dermatol.* **2016**, *28*, 645–647.
- (56) Chiang, Y. Z.; Pierone, G.; Al-Niaimi, F. Dermal fillers: pathophysiology, prevention and treatment of complications. *J. Eur. Acad. Dermatol. Venereol.* **2017**, *31*, 405–413.
- (57) Lee, C.; Shin, J.; Lee, J. S.; Byun, E.; Ryu, J. H.; Um, S. H.; Kim, D.-I.; Lee, H.; Cho, S.-W. Bioinspired, calcium-free alginate hydrogels with tunable physical and mechanical properties and improved biocompatibility. *Biomacromolecules* **2013**, *14*, 2004–2013.
- (58) Zhao, Q.; Mu, S.; Long, Y.; Zhou, J.; Chen, W.; Astruc, D.; Gaidau, C.; Gu, H. Tannin-tethered gelatin hydrogels with considerable self-healing and adhesive performances. *Macromol. Mater. Eng.* **2019**, *304*, No. 1800664.
- (59) Fan, H.; Wang, J.; Zhang, Q.; Jin, Z. Tannic acid-based multifunctional hydrogels with facile adjustable adhesion and cohesion contributed by polyphenol supramolecular chemistry. *ACS Omega* **2017**, *2*, 6668–6676.
- (60) Valachová, K.; Baňasová, M.; Topol'ská, D.; Sasinková, V.; Juránek, I.; Collins, M. N.; Soltés, L. Influence of tiopronin, captopril and levamisole therapeutics on the oxidative degradation of hyaluronan. *Carbohydr. Polym.* **2015**, *134*, 516–523.
- (61) Duan, J.; Kasper, D. L. Oxidative depolymerization of polysaccharides by reactive oxygen/nitrogen species. *Glycobiology* **2011**, *21*, 401–409.
- (62) Valachová, K.; Topol'ská, D.; Mendichi, R.; Collins, M. N.; Sasinková, V.; Soltés, L. Hydrogen peroxide generation by the Weissberger biogenic oxidative system during hyaluronan degradation. *Carbohydr. Polym.* **2016**, *148*, 189–193.